

Original Paper

## Test Method for SR Cracking of Welded Steels

Koreaki TAMAKI and Jippeï SUZUKI  
(Department of Mechanical and Materials Engineering)

(Received September 16, 1980)

The modified implant test was newly proposed in this paper as the suitable method for evaluating the sensitivity of stress relief cracking which has occasionally occurred in the welded zone of high strength steels. It was confirmed from the experimental results that the stress relief cracking sensitivity could be compared by the critical value of the initial restraint stress ( $\sigma_{AW-crit}$ ) obtained from the modified implant test. The modified implant test had the following merits in comparison with other stress relief cracking test. 1) The stress relief cracking sensitivity was numerically expressed. 2) The performance of the testing required a small amount of the tested material.

### 1. Introduction

It has been pointed out that the stress relief cracking (SR cracking) or the reheat cracking was occasionally observed in the welded zone of some Cr-Mo steels, such as 80 kg/mm<sup>2</sup> high strength steels (HT80) and heat resisting low alloy steels. The SR cracking is characterized by the followings.

- 1) It occurs in low alloy steels which contain the carbide forming elements, such as Cr, Mo, V, Ti and Nb.<sup>1)</sup>
- 2) It initiates along the boundaries of preexisting austenite grains in the heat affected zone.<sup>2)</sup>
- 3) It occurs during the stress relief heat treatment.

Many test methods have been proposed for evaluating the sensitivity of the SR cracking in the previous works. These test methods consist of 1) giving the weld thermal cycle to the tested steels, and producing the similar microstructure as that of the actual heat affected zone (HAZ), 2) developing the residual stress, and 3) heating to the temperature of the stress relief heat treatment,

and keeping at the temperature.

In this paper, the modified implant test method is newly proposed. In the case of this method, HAZ microstructure is simply simulated by the actual weld thermal cycle. But the control of the magnitude of the stress is difficult. Therefore the stress, which corresponds to the welding residual stress, is loaded by the mechanical method, as will be mentioned later, so that the stress can be optionally controlled. The original implant test method has been used for testing the cold cracking. The modified implant test apparatus is equipped with the furnace for stress relief heat treatment. And this method was tried to apply for the quantitative evaluation of the SR cracking sensitivity of the commercial high strength steels.

## 2. Materials and experiments

### 2.1 Chemical compositions of steel specimens

Table 1 shows the chemical compositions of four commercial high strength steels. HT80(A) and HT80(B) steels are the T-1 type Ni-Cr-Mo steels and HT80(P) steel is a chromium free, molybdenum steel. HT60 steel is typical of the in-sensitive steel to the SR cracking.

steel	wt%											
	C	Si	Mn	P	S	Cu	Ni	Cr	Mo	V	Nb	B
HT80(A)	0.12	0.26	0.89	0.012	0.006	0.25	1.04	0.57	0.33	0.04	-	0.002
HT80(B)	0.13	0.28	0.83	0.015	0.006	0.23	0.85	0.49	0.43	0.04	-	0.0012
HT80(P)	0.13	0.33	1.38	0.013	0.003	-	-	-	0.59	-	0.04	0.0012
HT60	0.15	0.30	1.27	0.018	0.005	-	-	-	-	0.03	-	-

### 2.2 Implant test specimens and apparatus for SR cracking test

The shapes of implant test specimens are shown in Fig.1. The same materials were used both for the implants and the backing plates for the commercial high strength steels.

Fig.2 shows the outline of the modified implant test machine for the SR cracking test. This apparatus consists of the followings;

- 1) restraining system, which is the same with the implant test machine for the cold cracking test
- 2) heating system consisting of electric furnace, transformer and self-acting regulator
- 3) measuring devices of stress and temperature; dynamic strain meter, thermocouple and recorder

Two types of machines were made for the

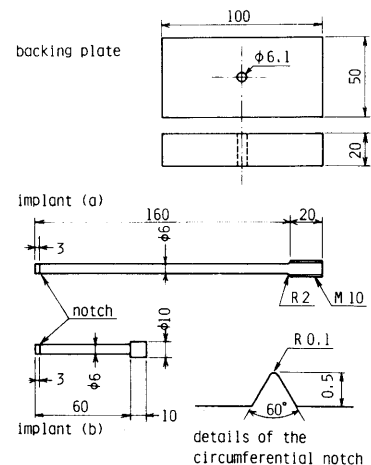


Fig.1 The shapes of implant test specimens

research of the SR cracking. Their details are illustrated in Fig.3 and Fig.4 respectively. For the first type machine, the implant in 180 mm length was used as shown in Fig.1-(a). The implant as shown in Fig.1-(b) was used for the second type machine. In the case of the second type machine, the loading was carried out with the lever to prevent the torsion, as shown in Fig.5. Two types of machines were the same in outline.

Welding was carried out using the D8016 electrode (4 mm in diameter) dried at 350°C for 1 hour.

The heat input was 17000 J/cm.

A given stress was loaded when the temperature of the HAZ fell down to 150°C. The heating began after 1 hour when the welding was finished. The specimen was heated at the rate of 200°C/hr up to 600°C, and then the temperature was held 600°C for 20 hours or until the implant was fractured. The stress relaxation

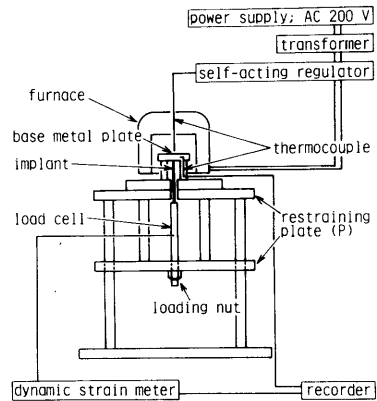


Fig.2 The outline of the modified implant test apparatus

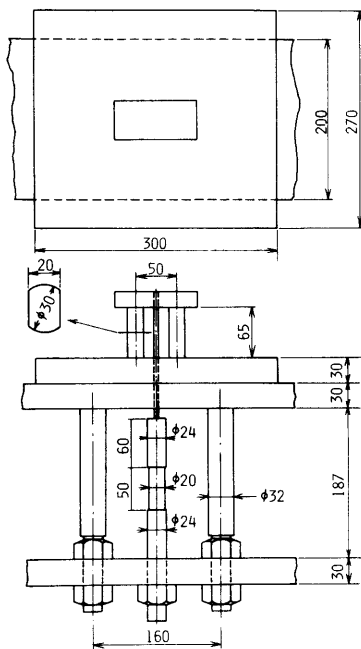


Fig.3 Details of the first type implant machine

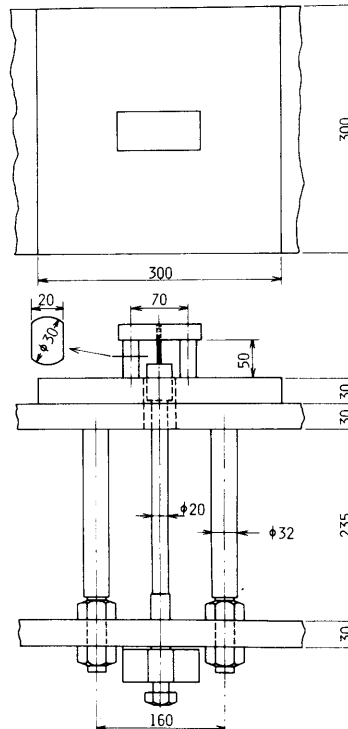


Fig.4 Details of the second type implant machine

curves were also drawn in the course of the heat treatment.

2.3 The terms representing the stress values

The following terms were used to distinguish the restraint stress loaded before or after the stress relief heat treatment.

- (a)  $\sigma_{AW}$ ; The initial restraint stress loaded just after the welding  
( briefly written as the initial restraint stress )
- (b)  $\sigma_{AW-crit}$ ; The critical value of the initial restraint stress to cause the SR cracking  
( briefly written as the critical restraint stress )
- (c)  $\sigma_{SR}$ ; The restraint stress during or after the stress relief heat treatment
- (d)  $\sigma_{SR-crit}$ ; The critical value of  $\sigma_{SR}$  to cause the SR cracking

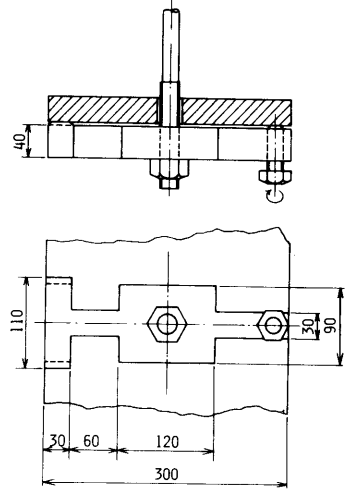


Fig.5 The lever for the loading of the second type machine

3. Test results on the commercial high strength steels

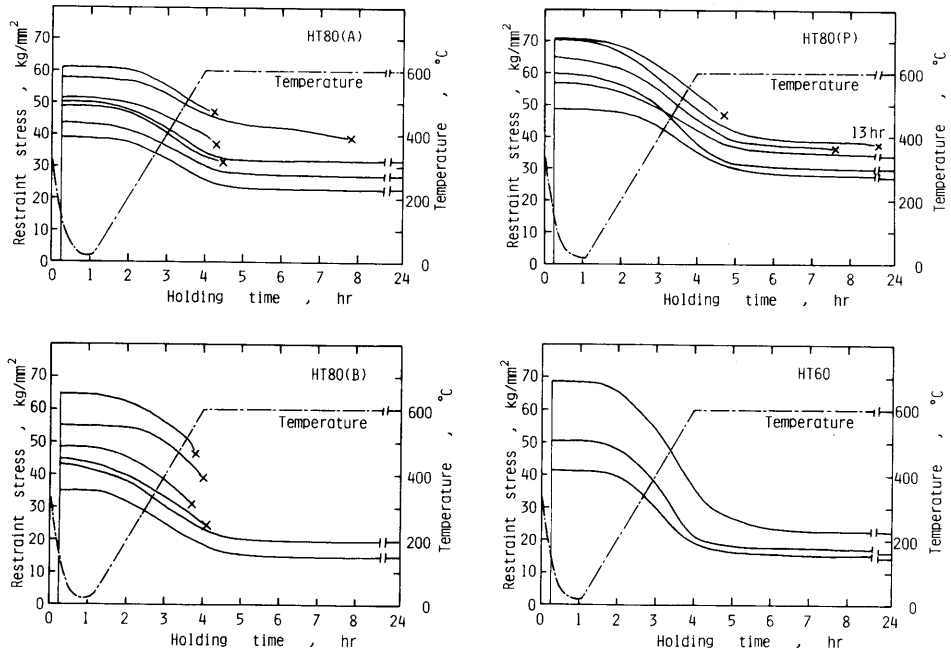


Fig.6 Stress relaxation curves of the commercial high strength steels, HT80 (A), (B), (P) and HT60 steels, obtained by the first type machine

The stress relaxation curves of HT80(A), (B), (P) and HT60 steels are shown in Fig.6. The symbol X in the figure shows the point on which the complete fracture occurred. From the results in the figure,  $\sigma_{AW-crit}$ ,  $\sigma_{SR-crit}$  and the stress relaxation are obtained, and tabulated in Table 2. The stress relaxation R is defined as the following equation.

$$R = \frac{\sigma_{AW} - \sigma_{SR}}{\sigma_{AW}} = 1 - \frac{\sigma_{SR}}{\sigma_{AW}} \quad (1)$$

R, which represents the degree of the decrease in the restraint stress, varied as a function of the holding time t, because of the change of  $\sigma_{SR}$ . However, R was considered to be a constant for each material even if the initial restraint stress  $\sigma_{AW}$  changed. and R varied scarcely after the temperature of the specimen reached 600°C. Therefore the value of R at 24 hours, R(24) can be considered to be a material constant. R(24) were shown in Table 2.

The T-1 type Ni-Cr-Mo steels (HT80(A) and (B) steels) are more sensitive to the SR cracking than the chromium free, molybdenum steel (HT80(P) steel). And HT60 steel is insensitive to the SR cracking. These results agree well to the SR cracking sensitivity estimated from the indexes,  $\Delta G^3$  and PSR<sup>4</sup>( shown as Table 2 ). It can be concluded from these experiments that the SR cracking sensitivity is numerically evaluated by the value of  $\sigma_{AW-crit}$  as the results of the modified implant test.

Table 2 Lists of  $\sigma_{AW-crit}$ ,  $\sigma_{SR-crit}$ , stress relaxation, PSR and  $\Delta G$

	$\sigma_{AW-crit}$ (kg/mm <sup>2</sup> )	$\sigma_{SR-crit}$ (kg/mm <sup>2</sup> )	stress relaxation at 24 hours ( % )	PSR	$\Delta G$
HT80(A)	47	29	38	-0.12	-0.017
HT80(B)	44	20	55	0.0	+0.233
HT80(P)	62	35	45	-0.54	-0.053

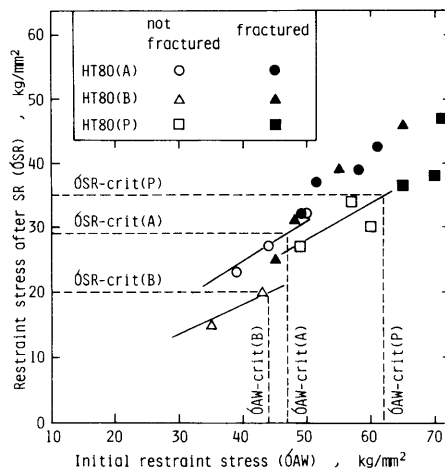


Fig.7 Diagram showing the relation between  $\sigma_{AW}$ ,  $\sigma_{AW-crit}$ ,  $\sigma_{SR}$  and  $\sigma_{SR-crit}$  on three types of HT80 steels

The relations between  $\sigma_{AW}$  and  $\sigma_{SR}$  are summarized in Fig.7. In the stress range in which the fracture did not occur,  $\sigma_{AW}$  and  $\sigma_{SR}$  were in proportion. Therefore the open marks are located on each straight line, the tangent of which corresponds to  $\sigma_{SR}/\sigma_{AW}$  in the stress relaxation formula (eq.(1)).

It will be seen that two factors influence  $\sigma_{AW-crit}$ . One of them is  $\sigma_{SR-crit}$ , and other is the stress relaxation. Because the stress relaxation R is not influenced by the value of  $\sigma_{AW}$ , the following equation is concluded.

$$R = \frac{\sigma_{AW} - \sigma_{SR}}{\sigma_{AW}} = \frac{\sigma_{AW-crit} - \sigma_{SR-crit}}{\sigma_{AW-crit}}$$

And then,

$$\sigma_{AW-crit} = \frac{\sigma_{SR-crit}}{1 - R}$$

For example, the value of the stress relaxation for HT80(P) steel is rather small but the  $\sigma_{SR-crit}$  of the steel is largest, and then the value of  $\sigma_{AW-crit}$  becomes the largest ( becomes insensitive to the SR cracking ). On the contrary, HT80(B) steel is most sensitive to the SR cracking in spite of the largest tendency of the stress relaxation.

4. Discussion for the test machine

4.1 The results of HT80(B) steel obtained by the second type machine

The critical restraint stress  $\sigma_{AW-crit}$  is influenced by the stress relaxation. Because the stress relaxation occurs in the cause of the plastic deformation of the implant, it can be expected that  $\sigma_{AW-crit}$  is influenced by the size of the implant specimen and the rigidity of the test machine. Fig.8 shows the stress relaxation curves of HT80(B) steel obtained by the second type machine.  $\sigma_{AW-crit}$  and  $\sigma_{SR-crit}$  were 35 and 21 kg/mm<sup>2</sup> respectively. The results

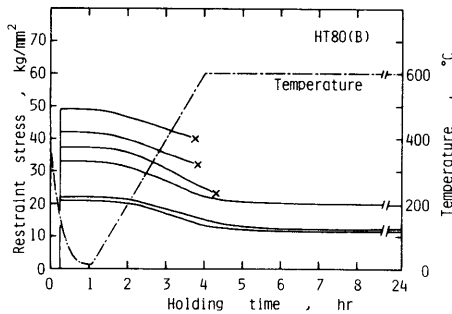


Fig.8 Stress relaxation curves of HT80(B) steel obtained by the second type machine

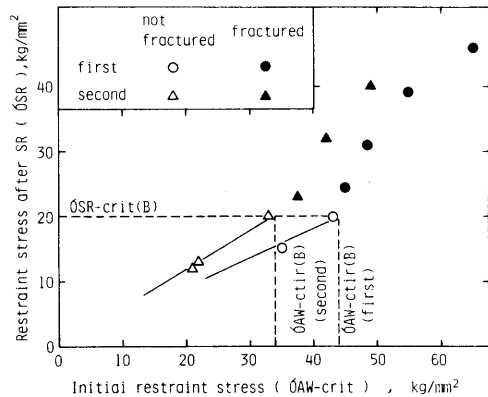


Fig.9 The comparison between the results of  $\sigma_{AW-crit}$  and  $\sigma_{SR-crit}$  obtained by two types of machines

are compared in Fig.9. As shown in Fig.9, there are the difference about  $10 \text{ kg/mm}^2$  between the values of  $\sigma_{AW-crit}$  obtained by two types of machines but the values of  $\sigma_{SR-crit}$  is the same. Therefore the difference in  $\sigma_{AW-crit}$  is due to the stress relaxation.

It was discussed that the relation between the quantity of the plastic deformation of the implant and the change of the force loaded to the specimen. The schematic illustration of the test machine is shown in Fig.10. When the load  $P$  is zero,

$$L = l_i + l_c \quad (2)$$

Where,  $l_i$  and  $l_c$  are the length of the implant and the load cell respectively, and

$L$  is the length of the test machine. When the load  $P_{AW}$  is applied,  $l_c$  decreases by the displacement of the loading nut,  $s$ . That is,

$$l_c' = l_c - s \quad (3)$$

Where,  $l_c'$  is the length of the load cell when  $P_{AW}$  is applied. Elastic elongations of the implant;  $\Delta l_i$ , the load cell;  $\Delta l_c'$  and the test machine;  $\Delta L$  are respectively

$$\Delta l_i = \frac{l_i}{E A_i} P_{AW} \quad \Delta l_c' = \frac{l_c'}{E A_c} P_{AW} \quad \Delta L = \frac{P_{AW}}{K} \quad (4)$$

Where,  $A_i$  and  $A_c$  are the area of the cross section of the implant and the load cell respectively.  $E$  is the elastic modulus and  $K$  is the rigidity of the test machine. Then, we find from eq.(2) and eq.(4)

$$\Delta l_i + \Delta l_c' + l_i + l_c' = \frac{l_i}{E A_i} P_{AW} + \frac{l_c'}{E A_c} P_{AW} + l_i + l_c' = L - \frac{P_{AW}}{K} \quad (5)$$

The plastic deformation of the implant occurs during the stress relief heat treatment and the load decreases from  $P_{AW}$  to  $P_{SR}$ . Then, elongations are

$$\begin{aligned} \Delta l_i(SR) &= \frac{l_i + x}{E A_i} P_{SR} + x \approx \frac{l_i}{E A_i} P_{SR} + x \quad (\because x \ll l_i) \\ \Delta l_c'(SR) &= \frac{l_c'}{E A_c} P_{SR} \quad \Delta L(SR) = \frac{P_{SR}}{K} \end{aligned} \quad (6)$$

Where,  $x$  is the quantity of the plastic deformation of the implant. Then, we find from eq.(2) and eq.(5)

$$\begin{aligned} \Delta l_i(SR) + \Delta l_c'(SR) + l_i + l_c' &= \frac{l_i}{E' A_i} P_{SR} + x + \frac{l_c'}{E A_c} P_{SR} + l_i + l_c' \\ &= L - \frac{P_{SR}}{K} \end{aligned} \quad (7)$$

Where,  $E'$  is the elastic modulus at the high temperature. From eq.(5) and eq.(7) the following equation is obtained, that is

$$x = \left( \frac{1}{K} + \frac{l_c'}{E A_c} \right) (P_{AW} - P_{SR}) + \frac{l_i}{A_i} \left( \frac{P_{AW}}{E} - \frac{P_{SR}}{E'} \right) \quad (8)$$

The values of  $K$  were determined by the experiment.

$$K_1 = 161.499 \text{ (kg/mm)} \quad (\text{the first type machine})$$

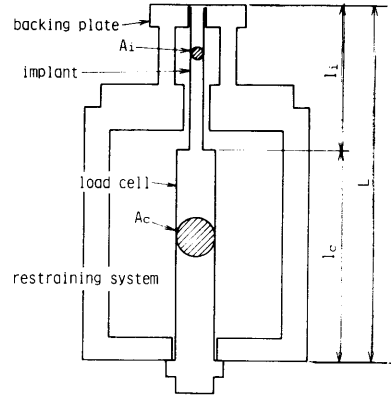


Fig.10 The schematic illustration of the test machine

$K_2 = 210.438$  (kg/mm) (the second type machine)

Substituting the actual values of  $l_i$ ,  $l_c'$ ,  $A_i$ ,  $A_c$ ,  $K$  and  $E$  into eq.(8), the following relations were obtained. That is,

$$x_1 = 6.228 \times 10^{-3} (P_{AW} - P_{SR}) + 5.659 \left( \frac{P_{AW}}{21000} - \frac{P_{SR}}{10200} \right) \quad (\text{the first type machine})$$

$$x_2 = 4.808 \times 10^{-3} (P_{AW} - P_{SR}) + 2.122 \left( \frac{P_{AW}}{21000} - \frac{P_{SR}}{10200} \right) \quad (\text{the second type machine}) \quad (9)$$

the first type machine;  $l_i = 160$ ,  $l_c' = 195$ ,  $A_i = 28.27$ ,  $A_c = 254.47$ ,  
 the second type machine;  $l_i = 60$ ,  $l_c' = 370$ ,  $A_i = 28.27$ ,  $A_c = 314.16$   
 $E = 21000$  (at room temperature),  $E' = 10200$  (at 600°C)

$x$  is divided into two parts. One is the deformation at the notch  $x_N$ , and other is the plastic strain  $e_p$  through the implant of 6 mm in diameter.

$$x = x_N + l_i e_p$$

In the case of the test under the critical restraint stress, it can be considered that the values of  $x_N$  and  $e_p$  are the same for both machines. Then,

$$x_1 = x_N + 160 e_p \quad (10)$$

$$x_2 = x_N + 60 e_p$$

Substituting the actual values of  $\sigma_{AW-crit}$  and  $\sigma_{SR-crit}$  into eq.(8), we obtained

$$x_1 = 2.949 \text{ (mm)}, \quad x_2 = 1.308 \text{ (mm)} \quad (11)$$

From (10) and (11)

$$x_N = 0.323 \text{ (mm)}, \quad e_p = 1.641 \times 10^{-2} \quad (12)$$

Fig.11 shows the result of measuring the plastic deformation of the implant using the first type machine. The experimental value of  $x_N$  was about 0.25 mm.

As discussed above, the stress relaxation characteristics is largely dependent on the combination of the rigidity of machine  $K$  and the length of the specimen  $l$ . Therefore, the selection of both values is important, and it should be performed on the basis of the stress relaxation characteristics in the actual weldment.

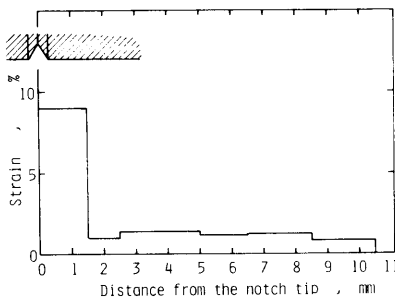


Fig.11 The result of measuring the plastic deformation of the implant (HT80(B),  $\sigma_{AW} = 40 \text{ kg/mm}^2$ , the first type machine)

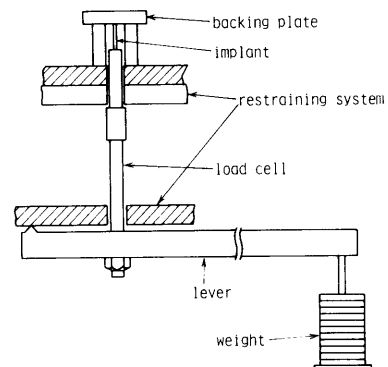


Fig.12 Mechanical loading system with the lever in the case of the dead weight test



4.2 SR cracking test under the constant load ( dead weight test )

The dead weight test machine is shown in Fig.12. The loading was carried out by the lever and the weight. The load was kept at the constant value during the stress relief heat treatment. The testing was made on HT80(B) steel. Testing conditions and welding parameters were the same as the previous experiments except the loading method. The results were shown in Fig.13 Any specimen fractured at the high temperature range, 570~590°C. Two types of fracture appeared in the fractured surface of the implant, as shown in Photo.1. Fractured surface, A was SR cracking because the fracture occurred along the grain boundaries of preexisting austenite and the plastic deformation was scarcely detected. Fractured surface, B was not SR cracking but the ductile fracture. The area of the ductile surface was measured, and the stress at the fracture  $\sigma_{true}$  was calculated. The resulting  $\sigma_{true}$  decreased with elevating the temperature at fracture, as shown in Fig.14. The value of  $\sigma_{true}$  will be considered to be the fracture

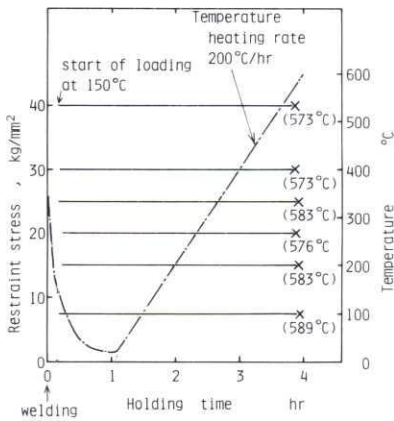


Fig.13 Results of the dead weight test  
note: ( x ) temperature at which the fracture occurred

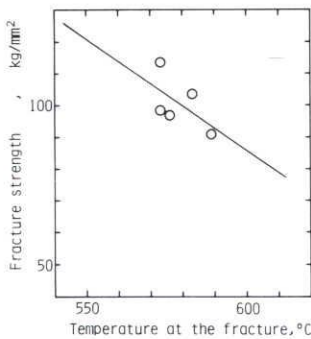
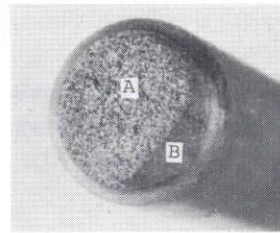


Fig.14 Relationship between the fracture strength and the temperature at the fracture



A; SR cracking



B; ductile fracture

Photo.1 The appearance of the fractured surface of the implant

strength of the material at the high temperature. In the case of the constant load method, the mechanism of the fracture was quite difference from that of previous experiments. Therefore this method can not be immediately applied for evaluation of the SR cracking sensitivity.

#### 5. Conclusions

The modified implant test machine was produced for the research of the SR cracking sensitivity of the steels. The results are summarized as follows.

(1) The SR cracking sensitivity is evaluated exactly by the critical restraint stress,  $\sigma_{AW-crit}$ , each of which is obtained by the same machine and the same specimen size.

(2) The  $\sigma_{AW-crit}$  is influenced by the value of  $\sigma_{SR-crit}$  and the stress relaxation. And the stress relaxation is dependent on the rigidity of the machine and the specimen size.

#### Acknowledgments

The authors wish to thank Associate Professor M.Kojima, Mr.T.Marui and the members of the working group on SR cracking in Mie university for their cooperative works.

#### References

- 1) Y.Ito and M.Nakanishi: J.J.W.S., Vol.40. (1971) No.12, 1261-1266
- 2) R.A.Swift: Welding J.Vol.50(1971), No.5, 195s-200s
- 3) T.Naiki and H.Okabayashi: J.J.W.S., Vol.39(1970) No.10, 1059-1066
- 4) Y.Ito and M.Nakanishi: J.J.W.S., Vol.41(1972) No.1, 59-64